MODELING OF COAL LIQUEFACTION WITH HINDERED DIFFUSION

Young-Woo Rhee* and James A. Guin

*Korea Institute of Energy Research, 71-2 Jang-dong, Yoosung-gu, Taejeon, Korea
Department of Chemical Engineering, Auburn University, Auburn, AL 36849, U.S.A.
(Received 27 October 1992 • accepted 26 December 1992)

Abstract—A simple model taking into account most important aspects of catalyst properties and reaction was developed to interpret a maximal point in catalyst activity observed using unimodal catalysts in coal-tetralin reactions. The model was found to be highly applicable to the prediction of catalyst activity and the maximal point in catalyst activity could be explained in terms of the trade-off between the hindered diffusion and surface area.

INTRODUCTION

Generally, in a catalyzed reaction as the catalyst surface area increases the reaction rates increase. However, in reactions with large molecules, such as coal liquefaction and petroleum hydroprocessing, a point may be reached where the catalyst pore size is so small as to significantly impede the diffusion rate, i.e. encounter the hindered diffusion regime. This trade-off between surface area and diffusional accessibility implies that there should be an optimum catalyst pore size, or pore size distribution, for reactions of this nature. The existence of such an optimum has been experimentally verified and analyzed by several investigators [1-3].

A method for minimizing the intraparticle diffusional resistance present in the hindered regime would be the utilization of macro-micro (bimodal) type catalysts, wherein macropores provide rapid non-hindered access to high surface area microporous regions. Catalysts such as these have shown promise for improved liquefaction performance [4-6]. Several questions remain, however, regarding the degree to which catalyst performance can be improved by pore structure modification. For example, it is not clear whether the advantages due to increased effective diffusivities in bimodal catalysts will be more than offset by their decreased volumetric surface area. Also, it is not clear whether a unimodal catalyst with, say, an average (medium) pore size will be more or less effective than a bimodal catalyst with a mixture of smaller and larger pores. Furthermore, it is likely that answers to these questions will be system dependent and will require additional information regarding reactant molecular sizes and reaction rates in order to judge the effectiveness of a particular catalyst.

Most studies dealing with catalyst pore structure effects on overall reaction rates have neglected to measure the intrinsic activity of the respective extrudate catalysts, thus making it difficult to categorize differences in performance due to transport phenomena from intrinsic surface activity effects. In this study, intrinsic catalyst activities of all extrudates were measured by grinding the catalyst to a fine powder (-150 mesh) to minimize intraparticle diffusion resistances.
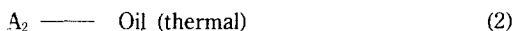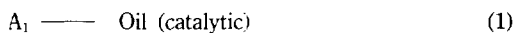
The objective of this study is to develop and apply a model within which the effects of catalyst physical properties, e.g. surface area, density, pore size distribution, etc. on coal liquefaction reactions can be evaluated. The model, thus developed, is then used to provide a framework for interpretation of reaction data from a series of catalytic reactions made with catalysts having several different pore size distributions. A great many models have been utilized to represent the kinetics of coal liquefaction [7-10]. Because the emphasis in this paper is on the variation in product yield with catalyst physical properties rather than the kinetics, a very simple kinetic model for the coal break-

*The author to whom correspondences should be addressed.

down process is adopted. Therefore, the conclusions reached concerning catalyst physical property effects will not be too dependent on the particular kinetic model adopted for coal liquefaction.

MODEL DEVELOPMENT

In particular, the coal is visualized as being composed of various species A_i with initial concentrations C_{Aio} which in turn form various products via a series of parallel reaction pathways.

$$A_1 \longrightarrow \text{Oil (catalytic)} \tag{1}$$

$$A_2 \longrightarrow \text{Oil (thermal)} \tag{2}$$

$$A_3 \longrightarrow \text{gas} \tag{3}$$

$$\vdots \qquad \qquad \vdots$$

An individual species A_i can be visualized as a part of the coal molecular structure which is most susceptible toward a particular mode of reaction, such as, conversion to gases, or thermal cracking to oil. The pentane soluble oil products are visualized as being formed by two reaction pathways which are catalytic and thermal, as shown in reactions 1 and 2, respectively. Reaction 1 is of main interest and the other reactions are postulated only to satisfy certain experimental observations. The initial concentrations of the various fractions would be dependent upon the particular coal being liquefied. In order to develop the necessary equations for exploring the effect of catalyst pore size distribution on the product yields, reaction 1 is rewritten for convenience as

$$A \xrightarrow{\ k_s\ } \gamma B \tag{4}$$

where A represents oil precursor molecules susceptible to catalytic liquefaction, including preasphaltenes and asphaltenes, B represents pentane soluble oil formed by catalytic reaction, and γ is a stoichiometric number. Pellet catalysts are assumed to have the simplest bimodal pore size distribution, i.e. two δ-functions. For a bimodal pore size distribution,

$$g(a) = N_1\ \delta(a - a_1) + N_2\ \delta(a - a_2) \tag{5}$$

where N_1 is the number of pores of area a_1 per unit volume of pellet and N_2 is the number of pores of area a_2 per unit volume of pellet. In this case the two properties ρ_s (solid density) and ρ_c (pellet density) completely define all other properties such as ε (porosity), S_v (surface area per unit pellet volume), S_g (sur-

face area per unit pellet weight) [11]. Eventually, the reaction rate based on pellet volume with first order kinetics becomes [11, 12],

$$r_v = - k_v\ C_A\ \eta \tag{6}$$

where the effectiveness factor η is a function of the Thiele modulus ϕ as shown in Eq. (7). In Thiele modulus, the effective diffusivity of reactant, D_e in the catalyst extrudates incorporates the effects of catalyst pore structure on the effective diffusion coefficient of the reactant.

$$\eta = \tanh\phi/\phi \tag{7}$$

where,

$$\phi = V_p/S_x(k_v/D_e)^{1/2} \\ = L_p(k_v/D_e)^{1/2} \tag{8}$$

Also, k_v is defined as follows.

$$k_v = S_g \rho_c k_s = S_v k_s \tag{9}$$

In the case of a finite cylindrical pellet, the characteristic length L_p i.e., V_p/S_x is expressed in terms of pellet diameter D and pellet length L as follows:

$$L_p = V_p/S_x = DL/(4L + 2D) \tag{10}$$

From the material balance in a batch reactor,

$$V_l \frac{dC_A}{dt} = r_v V_{cat} \\ = - k_v C_A \eta V_{cat} \tag{11}$$

or

$$\frac{dC_A}{C_A} = - k_v \eta m dt = - k_s m S_v \eta dt \tag{12}$$

where V_l = volume of liquid solvent in the reactor
$\qquad V_{cat}$ = volume of catalyst loaded
$\qquad m$ = volume ratio of catalyst to liquid solvent, V_{cat}/V_l

Solving for C_A in Eq. (12),

$$C_A = C_{Ao} \exp(- kt) \tag{13}$$

where k is expressed as follows,

$$k = k_v m \eta = k_s m S_v \eta \tag{14}$$

Eq. (12) indicates that the product yields obtained by using various catalysts having the same intrinsic surface activity (k_s = constant) depend on the product $m S_v \eta$. To the extent that $m S_v$ is constant, the variations in product yields for various catalysts can be attributed to differences in effectiveness factors.

The effectiveness factor η of a bimodal catalyst can be expected to increase because of two factors, i.e. a decrease in S_v and an increase in D_e. The first factor exists regardless of the diffusional mechanism, i.e. hindered or non-hindered; however the second factor is most significant in the hindered diffusion regime where $\lambda > 0.1$. These effects will reduce ϕ and increase η. Experiments comparing various catalysts are generally performed using either a constant mass, or a constant volume of catalyst. An increase in effectiveness factor for a bimodal vs. unimodal catalyst will be at least partly offset by the decline in S_v, if reactions are performed using a constant volume of catalyst (constant m) as indicated by Eq. (12). Thus, the product $S_v\eta$ on the right hand side of Eq. (12) may either increase or decrease upon changing from a unimodal to a bimodal catalyst. Conversely, if reactions are performed using a constant mass of catalyst, the factor mS_v, equal to the unit area of catalyst per unit volume of liquid, remains approximately constant and variations in product yields are roughly indicative of variations in η alone. The approximate invariance of mS_v in the case of reactions using a constant mass of catalyst is due to the fact that, when macropores are introduced into a unimodal microporous catalyst, S_g is roughly constant because most of the surface area is in the micropores.

Proceeding with the model development, the solution of the material balance, Eq. (12), yields as expression for the weight percentage of catalytically formed pentane soluble oils in the reaction mixture. The amount of product formed, N_B is directly obtained from the amount of reactant converted, N_A as shown in Eq. (15).

$$N_B = \gamma N_A \tag{15}$$

Therefore, the concentration of oils will be

$$Wt\%\ oil = \gamma\beta C_{Ao}[1 - exp(-kt)] \tag{16}$$

where the lumped rate constant k is given by Eq. (14) and β is a constant which converts the concentration data to a weight percentage basis. C_{Ao} is the effective concentration of oil precursor molecules in the coal which are susceptible to oil formation by the catalytic route shown in reaction 1. The combined constant $\gamma\beta C_{Ao}$ will be chosen to fit the available experimental data and is assumed to be the same for all catalysts studied here.

The effect of catalyst pore structure on the weight percent oils fraction enters Eq. (16) through the dependence of the effectiveness factor η. In order to relate the effective diffusivity D_e to the catalyst pore structure, a model for the pore geometry must be chosen. Considering the tortuous and highly interconnected pore structure of extrudate catalyst pellets, the parallel cross-linked pore model was adopted with completely communicating randomly oriented cylindrical pores as presented by Froment and Bischoff [12]. For a catalyst with groups of randomly oriented ($\tau = 3$) cylindrical pores of radii R_i and group void fractions ε_i the effective diffusivity is

$$D_e = \frac{D_m}{\tau} \Sigma\varepsilon_i F(\lambda_i) \tag{17}$$

In addition, the catalyst volumetric surface area is given by

$$S_v = 2\Sigma\varepsilon_i/R_i \tag{18}$$

In Eq. (17) the function $F(\lambda)$ represents the effects of hindered diffusion of a large molecule diffusing through small catalyst pores. This function depends on the ratio of molecule size to pore size, $\lambda_i = R_m/R_i$. It can be shown from simple model calculations that the tortuosity should be a function of the molecule to pore size [13]; however, it is difficult to incorporate this dependence because it depends on difficult-to-measure geometric properties of the pore structure. Most empirical equations developed for restricted diffusion have ignored this effect, thus essentially incorporating the dependence of τ on λ into the $F(\lambda)$ factor. This approach is taken here for the sake of simplicity and the following function $F(\lambda)$ is chosen from several which seem to fit the experimental data given by Chantong and Massoth [14], viz.,

$$F(\lambda) = (1 - \lambda)^2(1 - 2.104\lambda + 2.09\lambda^3 - 0.95\lambda^5) \tag{19}$$

Eq. (19) was theoretically developed for pores with a τ of unity; however, its qualitative behavior is roughly the same as other more empirical equations. The simplest pore model which can represent the bimodal features of the catalysts used in this work would consist of two distinct pore radii, R_1 and R_2, representing micro and macropores, respectively. In this case the summation in Eqs. (17) and (18) only extends to the two values i = 1, 2. In addition, it is considered for simplicity that the reactant molecules can be represented by a single molecular size, R_m. By relaxing these assumptions, the model formulated above can be extended to multiple reactions with arbitrary kinetics, arbitrary catalyst pore size distributions, and a continuous range of reactant molecular sizes; however, the resulting equations would, given the current state of

Table 1. Experimentally determined catalyst properties

Catalyst name	ε_1	ε_2	λ_2/λ_1	d_1 (angstroms)	S_ν (m²/cc)	m	V_p/S_x (cm)
G	0.58	a	a	55	422	0.066	0.084
I	0.62	a	a	85	294	0.065	0.083
C	0.46	a	a	105	173	0.065	0.077
D	0.02	0.34	0.199	215	14	0.049	0.068
J	0.54	0.07	0.036	56	388	0.075	0.085
K	0.36	0.36	0.026	61	245	0.108	0.092
Shell-324:							
0.8 mm	0.59	a	a	114	206	0.066	0.017
1.6 mm	0.59	a	a	111	212	0.067	0.030
3.2 mm	0.62	a	a	110	227	0.068	0.059
Shell-317							
3-lobe	0.57	0.14	0.048	107	218	0.093	0.022
Amocat-1C							
1.6 mm	0.50	0.19	0.046	121	175	0.100	0.032

a: Catalyst contains no macropores.

Table 2. Catalyst activity data

Catalyst name	Oils yield (wt%)	
	Pellets	Powder
None		35.2
G	42.3	77.5
I	52.5	78.4
C	49.2	74.8
D	35.9	41.2
J	54.9	75.8
K	57.8	74.5
Shell-324:		
0.8 mm	65.2	79.7[a]
1.6 mm	61.3	77.1
3.2 mm	57.2	81.6
Shell-317 3-lobe	69.9	80.0
Amocat-1C 1.6 mm	69.5	77.9

a: It was estimated by taking an average value of 77.1 and 81.6 wt% which were obtained using the other Shell-324 catalysts.

knowledge concerning catalytic coal liquefaction, be so complex as to lack utility. The first order model with a bimodal catalyst pore size distribution and single size molecular reactant is the simplest model capable of representing the qualitative features of interest in this paper.

To apply the model to the experiments performed herein, the experimentally measured properties shown in Table 1 were used. The equations formulated in the model development apply only to a catalytic reaction (reaction 1). Because some oil product (see Table 2 and reaction 2) is produced in a strictly thermal

Fig. 1. Flow chart for algorithm.

reaction with no catalyst present, the total pentane soluble oil in the products will be that from both the catalytic and thermal reactions. Since approximately 35.2 wt% oils are produced via the thermal route (see Table 2) the total wt% pentane soluble oils is given by

$$\text{Total wt\% oil} = \gamma\beta C_{Ao}[1-\exp(-kt)]+35.2 \qquad (20)$$

Eq. (20) will be used to analyze the experimental data by studying the effect of the catalyst properties on the lumped rate constant k. Once the values of k_s and $\gamma\beta C_{Av}$ are chosen, the calculation of total wt% oil will be straightforward as shown in Fig. 1.

In order to apply the model formulated in the pre-

Table 3. Effect of R_m on the coal liquefaction model

R_m	At optimum		
(angstroms)	k_s(cm/s)	$\gamma\beta C_{Ao}$(wt%)	σ(wt%)
0.1	4×10^{-9}	42	8.24
1	7×10^{-9}	45	3.17
5	3×10^{-8}	45	4.92
10	6×10^{-8}	45	7.46
15	5.9×10^{-7}	41	8.07
20	1×10^{-6}	41	8.33
25	3×10^{-6}	41	8.84

Table 4. Results of computer simulation for the coal liquefaction model

Catalyst name	$D_e \times 10^7$ (cm²/s)	η Pellet	Powder	$(S_vD_e)^{1/2}$ (cm/s)$^{1/2}$	Oils yield(wt%) Pellet	Powder
G	0.62	0.008	0.397	0.511	44.8	78.4
I	1.11	0.014	0.590	0.571	45.6	78.4
C	0.97	0.018	0.672	0.410	43.5	78.4
D	1.30	0.083	0.969	0.135	37.7	57.1
J	0.85	0.010	0.476	0.574	46.9	78.4
K	1.80	0.017	0.725	0.663	51.7	78.4
Shell-324:						
0.8 mm	1.31	0.085	0.697	0.519	65.6	78.4
1.6 mm	1.28	0.047	0.688	0.522	57.2	78.4
3.2 mm	1.34	0.024	0.683	0.552	49.3	78.4
Shell-317	1.74	0.073	0.740	0.616	69.6	78.4
Amocat-1C	1.91	0.059	0.792	0.578	64.1	78.4

ceding development, a number of catalyst physical properties were measured and are summarized in Table 1. The pentane soluble oil fraction from catalytic reaction experiments is also given in Table 2. The tortuosity factor τ was chosen to equal 3, the value for a randomly oriented pore structure; values of 2 to 7 are reasonable for catalysts of this type [15].

The molecular diffusivity D_m was estimated using the Stokes-Einstein equation [16], i.e.

$$D_m = \frac{k_B T}{6\pi\mu R_m} \qquad (21)$$

The viscosity of solvent tetralin, μ was roughly estimated using the thermodynamic data. At the experimental conditions of this study, i.e. 425°C and 86 atm the viscosity of tetralin was ca. 0.063 cp. The reaction model also contains certain parameters, namely R_m, $\gamma\beta C_{Ao}$, and k_s which were not directly measured.

There is presently some uncertainty regarding the exact nature and size of macromolecules such as asphaltenes in coal liquids. It would be very hard to select a molecule size representing coal because of its complex composition. For simplicity, coal derived asphaltenes were considered in this model as the typical molecules representing coal. Published data [17, 18] for the molecular weight of coal asphaltenes range from approximately 400 to 800, which vary considerably depending upon the method of measurement. The size of coal derived asphaltenes can be estimated from the molecular weight data. The typical molecular size representing coal was chosen as 7 angstroms. The remaining two parameters in the model, k_s and $\gamma\beta C_{Ao}$ were chosen by a least squares fit of the wt% oil data for both pellet and powdered catalysts.

RESULTS AND DISCUSSION

The algorithm for the computer simulation is shown in Fig. 1, where the model parameters, i.e., k_s, $\gamma\beta C_{Ao}$ are determined via an iteration loop to minimize the

standard deviation σ between the model and experiment. The data for the computer simulation, which were experimentally determined in the Auburn University Coal Research Laboratory are listed in Tables 1 and 2. The detailed experimental procedure has been already described by Rhee et al. [2].

In Table 1, 4.8 mm (3/16 inch) noncommercial catalysts G, I, C, D, J, and K were prepared in the laboratory using both double impregnation by incipient wetness (for catalysts C and D) and coextrusion (for catalysts G, I, J and K) techniques. Nickel nitrate and ammonium molybdate were used as active catalyst components of which amounts were adjusted to give ca. 3 wt% nickel oxide and 15 wt% molybdenium oxide in the final metal oxide catalyst. Complete details regarding catalyst preparation are given by Rhee [11].

As shown in Table 3, the size of reactant (R_m) has a significant effect on the model. A minimum standard deviation exists at ca. one angstrom of R_m; however, the selection of this low molecular size as R_m would be unrealistic as discussed elsewhere.

Results of the computer simulation listed in Table 4 show that the simulated values of D_e agreed well with catalyst pore structures. Bimodal catalysts K and D showed high values of diffusivity among 4.8 mm catalysts, mainly due to their large macroporosity. For the same reason, bimodal catalyst J which has low macroporosity gave low diffusivity. The effective diffusivity in 3/16 inch unimodal catalyst G, I, and D was strongly dependent upon the size of micropore. As the pore size in Table 1 increased, the effective diffusivity in Table 4 increased. The importance of bimodality on the diffusivity was further evidenced in the commercial catalysts. As shown in Table 4, the
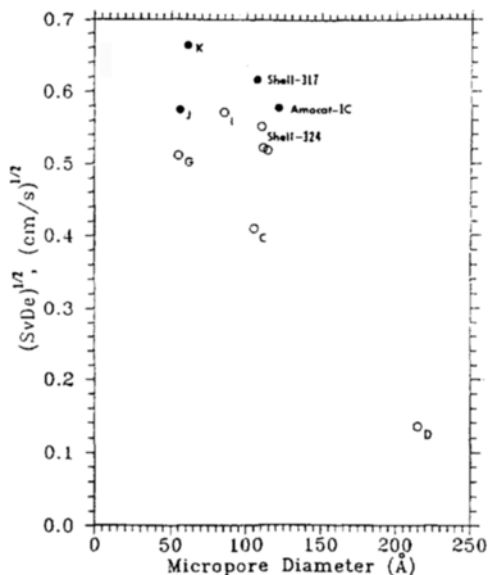
Fig. 2. Effect of average micropore size on catalyst activity in terms of $(S_vD_e)^{1/2}$ in the coal liquefaction model.

Fig. 3. Effect of surface area on catalyst activity in terms of $(S_vD_e)^{1/2}$ in the coal liquefaction model.

two commercial bimodal catalysts, i.e. Shell-317 and 1.6 mm (1/16 inch) Amocat-1C have higher diffusivities than those of unimodal Shell-324 catalysts. The results of both 4.8 mm bimodal (J and K) and commercial bimodal catalysts indicate that the amount of macroporosity has a significant effect on the effective diffusivity.

The low values of the effectiveness factor for pellet catalysts indicate that the reactions occur in the diffusion limited regime. The effect of catalyst pellet size on η was clearly observed in Shell-324 catalysts; as the pellet size increased from 0.8 to 3.2 mm, the effectiveness factor decreased almost proportionally. Also the commercial pellet catalysts showed higher values of the effectiveness factor than those of 4.8 mm catalysts mainly due to their smaller particle sizes. It is interesting to note that the effectiveness factor for powdered catalysts ranges from 0.40 for catalyst G to 0.97 for catalyst D, which suggests that the size of powder (−150 mesh, i.e. 0.105 mm in diameter) is still large enough to encounter diffusional limitations in coal liquefaction.

The effect of pore structure on the reaction rate k was more quantitatively investigated as shown in column 5 of Table 4. Since the effectiveness factor will approach 1/φ in the diffusion controlled regime, the reaction rate constant k can be rewritten from Eq. (14) as follows:
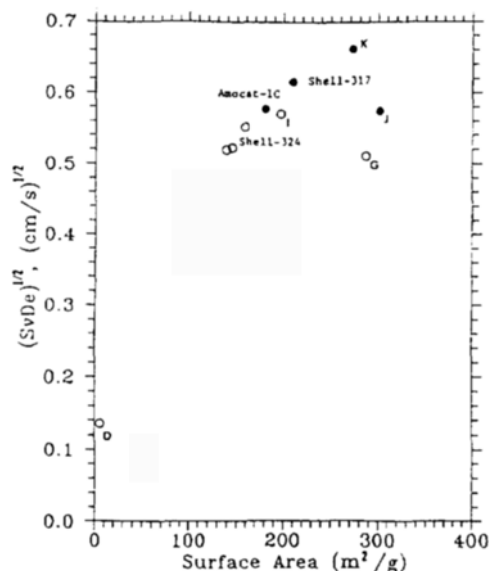
$$k = (k_s^{1/2}m/L_p)\ (S_vD_e)^{1/2} \qquad (22)$$

In Eq. (22), the intrinsic reaction rate constant k_s is assumed to be constant for all catalysts and two other parameters m and L_p are independent of the catalyst pore structure. Therefore, the effect of pore structure on the reaction rate constant is directly related to the surface area and effective diffusivity, i.e. $(S_vD_e)^{1/2}$. As shown in Figs. 2 and 3 where $(S_vD_e)^{1/2}$ is plotted against either micropore diameter or surface area, a maximal point exists for the unimodal catalysts. These results provide a theoretical explanation for the experimental data listed in Table 2 in terms of a trade-off between surface area and effective diffusivity. As the pore size increases, the surface area decreases while the effective diffusivity increases. Eventually, the combination of these two opposite effects will produce a maximal point. Interestingly the maximal point occurs at the micropore diameter of 78 angstroms which corresponds to $\lambda_1 = 0.18$. This specific value of λ_1 can be mathematically solved for unimodal catalysts because $(S_vD_e)^{1/2}$ is a function of only λ_1.

As shown in Figs. 2 and 3, bimodal catalysts give a higher reaction rate constant in terms of $(S_vD_e)^{1/2}$ than do unimodal catalysts. This higher value for bimodal catalysts is mainly due to the increase in the effective diffusivity. Obviously, the insertion of macropores into the catalysts reduced the surface area; however, the increase in the effective diffusivity more than compensates for the decrease in the surface area. The results shown in Figs. 2 and 3 imply that in design-
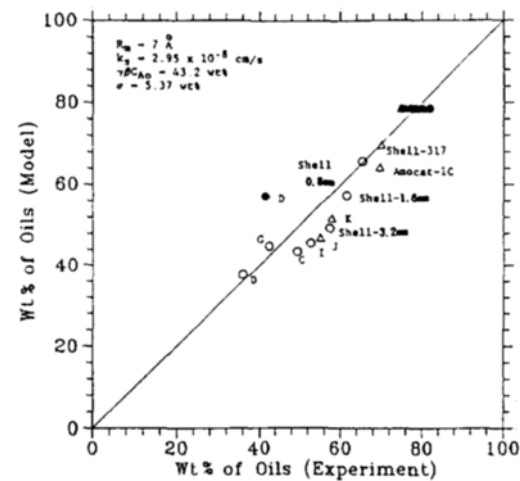
Fig. 4. Comparison of catalyst activity in terms of oils yield obtained from experiment and model work.

Table 5. Results of parameter sensitivity study in the coal liquefaction model with $R_m = 7$ angstroms

k_s	At optimum	
(cm/s)	$\gamma\beta C_{A_o}$(wt%)	σ(wt%)
2.95×10^{-10}	65	25.45
2.95×10^{-9}	54.2	10.27
2.95×10^{-8}	43.2	5.37
2.95×10^{-7}	36.2	9.01
2.95×10^{-6}	35	12.79

ing the optimal catalyst pore structure the micropore should be determined mainly by the reactant size while the size and amount of macropores should be chosen to keep the effective diffusivity large without an appreciable decrease in the surface area.

The simulated oil yields are listed in the last two columns of Table 4. As shown in Fig. 4, the model gives a good fit with a standard deviation of 5.33 wt%. The value of $\gamma\beta C_{A_o}$ which indicates a maximal oils yield converted via the catalytic reaction at the given reaction conditions is reasonably 43.2 wt%. The other model pararmeter k_s has a value of 2.95×10^{-8} cm/s. At this point it is difficult to discuss the significance of k_s value because of the lack of kinetic data. However, it compares well with the literature data [19].

As shown in Table 5, the order of magnitude in k_s value was varied to investigate the sensitivity of model parameters. Each $\gamma\beta C_{A_o}$ value was determined at an optimal condition where the standard deviation σ had a minimum value. The results show that the standard deviation is sensitive to the model parame-
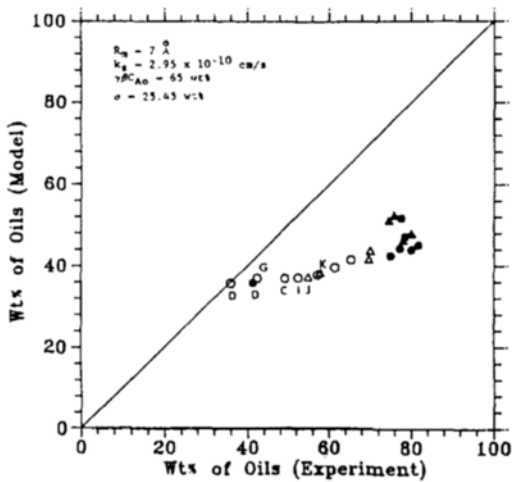

Fig. 5. Result of sensitivity study in the coal liquefaction model with $k_s = 0.01$ $(k_s)_{opt}$.
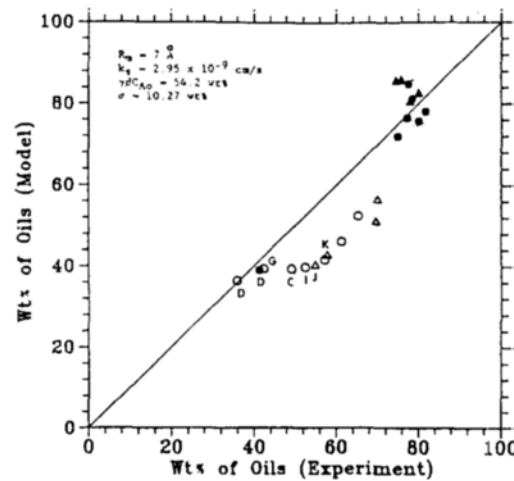

Fig. 6. Result of sensitivity study in the coal liquefaction model with $k_s = 0.1$ $(k_s)_{opt}$.

ters. In other words, the optimal point is very distinctive in itself.

As can be seen in Figs. 4-8, the variation in the order of k_s value caused a large deviation from the diagonal line, which represents the case of perfect agreement between the model and experimental data. In the graphs of model work, the filled symbols denote the data for powdered catalysts; the open symbols for pellet catalysts; the triangle symbol is used for bimodal catalysts; and the circle symbol for unimodal catalysts.

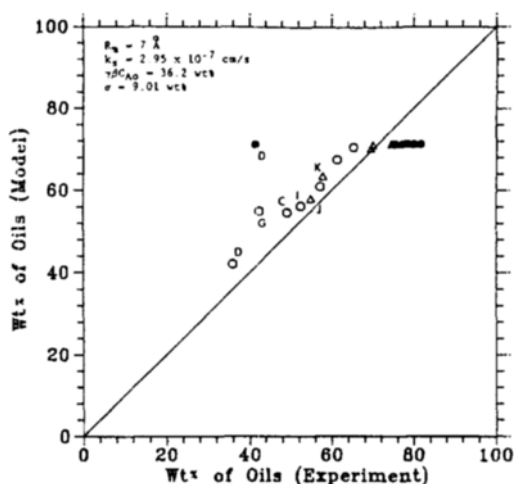In order to investigate the significance of $F(\lambda)$ defi-

Fig. 7. Result of sensitivity study in the coal liquefaction model with $k_s = 10$ $(k_s)_{opt}$.
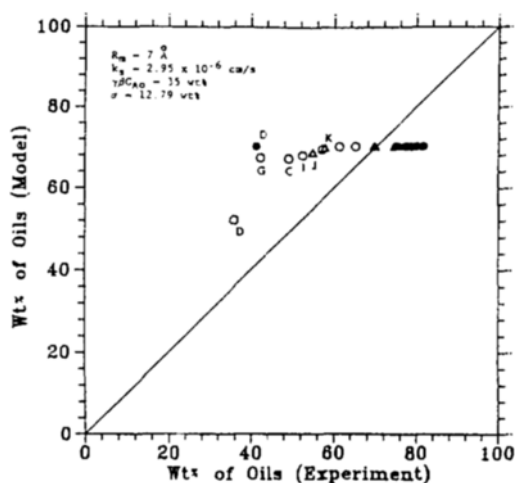

Fig. 8. Result of sensitivity study in the coal liquefaction model with $k_s = 100$ $(k_s)_{opt}$.

Table 6. Results of computer simulation for the coal liquefaction model with $F(\lambda) = 1$

Catalyst name	$D_e \times 10^7$ (cm²/s)	η		Oils yield(wt%)	
		Pellet	Powder	Pellet	Powder
G	2.24	0.019	0.727	49.4	78.2
I	2.39	0.024	0.800	47.7	78.2
C	1.77	0.029	0.833	44.5	78.2
D	1.39	0.102	0.979	37.4	52.3
J	2.35	0.020	0.751	50.6	78.2
K	2.78	0.025	0.846	52.3	78.2
Shell-324:					
0.8 mm	2.28	0.133	0.843	67.1	78.2
1.6 mm	2.28	0.075	0.839	58.9	78.2
3.2 mm	2.39	0.038	0.836	50.6	78.2
Shell-317	2.74	0.109	0.858	70.2	78.2
Amocat-1C	2.74	0.084	0.882	64.1	78.2

Fig. 9. Comparison of catalyst activity in the coal liquefaction model with $F(\lambda) = 1$.

ned in Eq. (19), $F(\lambda)$ was considered to be unity, i.e. which means the absence of hindered diffusion. The results shown in Table 6 and Fig. 9 imply that the introduction of $F(\lambda)$ into the model does not necessarily give a better interpretation of the experimental data. In addition, the model has been applied to the investigation of catalyst deactivation. All catalyst pores are assumed to be uniformly reduced during the catalyst deactivation. The uniform coating thickness ranges from 0 to 10 angstroms to observe its effects on the catalyst deactivation. According to the simulation results, the catalyst with larger micropores is less sensitive to the change in thickness compared to that

with smaller micropores. Also, bimodal catalysts with large amount of macropores have less sensitivity to the pore shrinkage than do unimodal catalysts.

From the simulation results, it is concluded that the high effective diffusivity results mainly from the large amount of macropores or large micropores, thus effecting high reactivity and slow deactivation. These macropores ensure the slow deactivation unless the catalytic surface area is drastically reduced due to their existence.

The main advantage of the model developed here is its simplicity; there is only one adjustable parameter, k_s. Nevertheless, the crucial experimental parameters were taken into account by this model. These

include catalyst shape (length and diameter), catalyst pore structure (bimodality, porosity, pore size), and other important properties such as density, tortuosity, and surface area. Additionally, the model takes into account the size of the reactant molecule.

In discussing the drawbacks of this model, it should be noted that the model is based on several assumptions as follows: (1) The pores perfectly communicate with each other; the tortuosity is 3; (2) The pore size distribution is two delta functions; (3) A first order irreversible reaction occurs; (4) The reactant is treated as one species of uniform size; and (5) Oil yield is considered to be the main objectives and fully represent the catalyst activity.

However, in reality the following problems occur: (1) The pores do not perfectly communicate with each other; the tortuosity is dependent upon the type of catalyst; (2) The pore has a complicated specific distribution; (3) Many reactions are involved; (4) Reactants consist of various molecules of different size; (5) The products are not one species and the catalyst activity is incorrectly represented by one product.

In spite of the limitations of the model, it still has a strong applicability due to its simplicity and its ability to fit experimental data. Therefore, the activity of any pellet catalyst could be effectively predicted only if a handful of simplified experimental parameters are given such as average pore diameters, porosities, surface area per pellet volume, characteristic pellet length, liquid volume ratio of catalyst pellet to solvent, and average reactant molecule size.

CONCLUSION

A simplified model describing the diffusion and reaction processes was developed to fit the catalyst activity data. The model was applied to interpret the oils yield data in the coal-tetralin reaction system. Despite its simplicity, the model turned out to be highly applicable to the prediction of pellet catalyst activity by taking into account the most important aspects of catalyst properties and reaction.

ACKNOWLEDGEMENT

NOMENCLATURE

a : cross sectional area of a pore [cm^2]

A : reactant
B : product
C_A : concentration of reactant [mole/l]
D : average diameter of catalyst pellet [cm]
D_e : effective diffusivity [cm^2/s]
D_m : molecular bulk diffusivity [cm^2/s]
F : combined function of K_r and K_p
g : pore size distribution function
K_p : steric coefficient
K_r : frictional drag coefficient
k : overall reaction rate constant [s^{-1}]
k_B : Boltzmann constant
k_s : surface reaction rate constant [cm/s]
k_v : volume reaction rate constant [s^{-1}]
L : average length of catalyst pellet [cm]
L_p : characteristic pellet length [cm]
m : volume ratio of catalyst to liquid [V_{cat}/V_l]
N : number of pores of area A per unit pellet volume [#/cc]
$N's$: amount of component [mole]
R : average pore radius [cm]
R_m : size of diffusing species [cm]
r_v : reaction rate based on pellet volume [mole/cc-s]
S_g : surface area per unit pellet weight [cm^2/g]
S_v : surface area per unit pellet volume [cm^{-1}]
S_x : characteristic surface area of pellet [cm^2/g]
t : time [s]
T : temperature [K]
V_{cat} : volume of catalyst loaded [cc]
V_l : volume of liquid in the reactor [cc]
V_p : characteristic pellet volume [cc/g]

Greek Letters

β : constant
ϵ : porosity
γ : stoichiometric number
η : effectiveness factor
λ : ratio of molecule radius to pore radius
μ : viscosity of solvent [cp]
ρ_c : pellet density (apparent density) [g/cc]
ρ_s : solid density (true density) [g/cc]
σ : standard deviation
τ : tortuosity
ϕ : Thiele modulus

Subscripts

1 : for micropores
2 : for macropores
i : for component i; for initial condition at t=0
o : for initial values at t=0

REFERENCES

1. Do, D. D.: *AIChE J.*, **30**, 849 (1984).
2. Rhee, Y. W., Guin, J. A. and Curtis, C. W.: *Energy & Fuels*, **3**(3), 291 (1989).
3. Ruckenstein, E. and Tsai, M. C.: *AIChE J.*, **27**, 697 (1981).
4. Alpert, S. B., Wolk, R. H., Marunic, P. and Chervenak, M. C.: U.S. Patent 3,630,888 (Dec. 1971).
5. Shimada, H., Kurita, M., Sato, T., Yoshimura, Y., Kawakami, T., Yoshitomi, S. and Nishijima, A.: *Bull. Chem. Soc. Japan*, **57**, 2000 (1984).
6. Shimura, M., Shiroto, Y. and Takeuchi, C.: *Ind. Eng. Chem. Fundam.*, **25**, 330 (1986).
7. Cronauer, D. C., Shah, Y. T. and Ruberto, R. G.: *Ind. Eng. Chem. Process Des. Dev.*, **17**, 281 (1978).
8. Mohan, G. and Silla, H.: *Ind. Eng. Chem. Process Des. Dev.*, **20**, 349 (1981).
9. Shah, Y. T., Cronauer, D. C., Mclivried, H. G. and Paraskos, J. A.: *Ind. Eng. Chem. Process Des. Dev.*, **17**, 288 (1978).
10. Shalabi, M. A., Baldwin, R. M., Bain, R. L., Gary, J. H. and Gelder, J. O.: *Ind. Eng. Chem. Process Des. Dev.*, **18**, 474 (1979).
11. Rhee, Y. W.: Ph.D. Dissertation, Auburn University, 1989.
12. Froment, G. F. and Bischoff, K. B.: "Chemical Reactor Analysis and Design", Wiley, New York, 1979.
13. Smith, D. M.: *AIChE J.*, **32**, 1039 (1986).
14. Chantong, A. and Massoth, F. E.: *AIChE J.*, **29**, 725 (1983).
15. Satterfield, C. N.: "Heterogeneous Catalysis in Practice", McGraw-Hill Book Company, 1980.
16. Reid, R. C., Prausnitz, J. M. and Sherwood, T. K.: "The Properties of Gases and Liquids", 3rd ed., McGraw-Hill Book Company, New York, 1977.
17. Bockrath, B. C. and Noceti, R. P.: *Fuel Processing Technol.*, **2**, 143 (1979).
18. Bockrath, B. C. and Schweighardt, F. K.: Advances in Chemistry Series, 195, ACS, Washington D.C. (1981).
19. Gollakota, S. V., Guin, J. A. and Curtis, C. W.: *Ind. Eng. Chem. Process Des. Dev.*, **24**, 1148 (1985).